Title

Magnetic coupling of vortices in a two-dimensional lattice

Journal

Nanotechnology, 26(46)

ISSN

0957-4484

Authors

Nissen, D

Mitin, D

Klein, O

et al.

Publication Date

2015-11-20

DOI

10.1088/0957-4484/26/46/465706

Magnetic coupling of vortices in a two-dimensional lattice

D. Nissen[1], D. Mitin[1], O. Klein[1], S. S. P. K. Arekapudi[2], S. Thomas[3], M.-Y. Im[4], P. Fischer[4,5], and M. Albrecht[1]

[1]Institute of Physics, University of Augsburg, 86159 Augsburg, Germany
[2]Institute of Physics, Chemnitz University of Technology, 09107 Chemnitz, Germany
[3]Materials Science and Technology Division, National Institute for Interdisciplinary Science and Technology, 695015 Thiruvananthapuram, India
[4]Center for X-ray Optics, Lawrence Berkeley National Laboratory, Berkeley, CA 94720, USA
[5]Physics Department, University of California, Santa Cruz, CA 94056, USA

[#]*Author to whom correspondence should be addressed: dennis.nissen@physik.uni-augsburg.de*

Abstract

We investigated the magnetization reversal of magnetic vortex structures in a two-dimensional lattice. The structures were formed by permalloy (Py) film deposition onto large arrays of self-assembled spherical SiO_2-particles with a diameter of 330 nm. In particular, we present the dependence of the nucleation and annihilation field of the vortex structures as a function of the Py layer thickness (aspect ratio) and temperature. By increasing the Py thickness up to 90 nm or alternatively by lowering the temperature the vortex structure becomes more stable as expected. However, the increase of the Py thickness results in the onset of strong exchange coupling between neighboring Py caps due to the emergence of Py bridges connecting them. We studied the influence of magnetic coupling locally by in-field scanning magneto-resistive microscopy and full-field magnetic soft x-ray microscopy, revealing a domain-like propagation process of vortex states with reducing in-plane magnetic field.

Introduction

Magnetic nanostructures have attracted large interest due to their unique properties. In this regard, as the size of a magnetic structure is reduced, the multi-domain state becomes energetically unfavorable and either a single domain or an inhomogeneous magnetization configuration is formed. In particular, for soft ferromagnetic disks in the micron size range a so called vortex state is favored, where the magnetization is forming an in-plane flux closure structure to minimize the magnetostatic energy [1-6]. This magnetic in-plane configuration can rotate clockwise (CW) or counter-clockwise (CCW). In addition, in the center, a vortex core occurs where the magnetization is pointing perpendicular to the disk plane as a result of minimizing the exchange energy [3, 7]. In general, the magnetic hysteresis curve of a magnetic vortex structure is characterized by two transitions in magnetization. Starting from a positive in-plane saturated state, the first transition occurs when a vortex is nucleated at the edge of the disk at a critical field called nucleation field (H_{nu}). By reducing further the field, the vortex core shifts perpendicular to the applied field from the edge to the center of the disk resulting in a zero net in-plane magnetization [8]. The movement of the core, up or down perpendicular to the applied field, depends on the sense of rotation of the in plane flux closure (circulation). At a certain negative field, a second transition occurs where the vortex vanishes accompanied by a sudden increase in magnetization. This critical field is called annihilation field (H_{an}). Recent studies have shown that the temperature has a large impact on the reversal process of individual disk structures [9-11]. In particular, for low temperatures the reversal process is guided by thermal activation [9], whereas for higher temperatures the reversal is implied by the temperature dependence of the saturation magnetization [9, 11]. Furthermore, the dynamics of both vortex core motion by means of rf-magnetic fields [12-16] and vortex switching by spin-polarized electric current [17-20] or by local fields [21-25] were studied experimentally and theoretically. Moreover, vortex oscillations have been studied in pair-coupled vortices [26–29], in one-dimensional vortex chains [30], and larger two dimensional vortex arrays [31–36]. In this regard, dipolar coupling will occur in particular when the center-to-center distance of a pair of vortices is less than twice the diameter of the disks [37, 38], which give rise to the appearance of these collective excitation modes [34, 36, 39].

In this study, a two dimensional vortex lattice was prepared by magnetic film deposition onto self-assembled densely packed particle arrays forming magnetic cap structures [25, 40-45]. Strong coupling is induced by deposition of thick Py films, where neighboring caps will be interconnected at the contact areas, resulting in direct magnetic exchange coupling. Here, we report on the influence of magnetic coupling on the reversal behavior and the in-plane circulation orientation of neighboring caps, which can lead to frustration in a hexagonal cap array [44, 45] or even to unexpected magnetization configurations.

Experimental

We use a simple bottom-up approach to realize arrays of magnetic vortex structures. This approach is based on self-assembly of spherical silica particles [46] with a diameter of 330 nm followed by deposition of a magnetic permalloy (Py: $Ni_{81}Fe_{19}$) thin film onto the particle array forming Py cap structures [41-44]. Here we focus on the influence of magnetic coupling on the magnetic properties induced by varying the Py film thickness between 20 - 130 nm. All films were deposited by dc-magnetron sputter deposition in a chamber with a base pressure of about 5 x 10^{-7} mbar. During deposition the Ar pressure was adjusted to 3.5 x10^{-3} mbar and the thickness was monitored using a quartz balance crystal. The Py layer was grown on a 5-nm-thick Ta layer to benefit the growing conditions and covered by a further Ta layer to prevent oxidation.

The morphology and the structure of the samples were characterized by scanning electron microscopy (SEM) and by cross section transmission electron microscopy (TEM). In order to probe the magnetic properties of the Py caps, magneto-optical Kerr effect (MOKE) magnetometry in longitudinal configuration was used to measure in-plane magnetic hysteresis loops. In this case, focusing optics were employed to reduce the diameter of the diode laser (λ = 670 nm) beam spot to about 3 μm on the sample thus the signal is averaged over about 100 Py caps. For temperature dependent measurements additionally a liquid nitrogen cryogenic sample stage was used, which allows measurements in the temperature range between 77 K and 500 K. Furthermore, direct observation of vortex structures was carried out using full-field magnetic transmission soft x-ray microscopy (MTXM) at the Advanced Light Source (beamline 6.1.2.) in Berkeley (USA), enabling real-space magnetic images with high-spatial resolution down to 20 nm [47]. In MTXM, magnetic contrast is given by x-ray magnetic circular dichroism, arising from the dependence of the x-ray absorption coefficients on the orientation between magnetization and photon helicity [47]. Magnetic imaging of Py caps was performed at a photon energy corresponding to the Fe L_3 (707 eV) x-ray absorption edge. To record images of in-plane magnetizations, specifically the circulation in the Py caps, the sample was mounted at 60° angles with respect to the x-ray propagation direction. In order to reduce non-magnetic background for the in-plane images, images taken at certain fields were normalized to an image recorded in the fully saturated state. Within an exposure time of a few seconds, an area of 30×30 caps can be imaged. In a further study, the vortex cores were investigated by an in-field scanning magnetoresistive microscope (SMRM) [25, 48]. This device uses a state-of-the-art magnetic recording head of a hard disk drive, which contains a tunneling magnetoresistive (TMR) read element, which is sensitive to the perpendicular component of the magnetic stray field above a vortex structure. Please note that this method allows magnetic imaging without influencing the magnetization state of the specimen. Thus individual vortex cores can be investigated and their lateral displacement when an in-plane field is applied can be evaluated.

Results

A typical SEM and a cross section TEM image of an array of particles covered by a 70-nm-thick Py film is shown in Fig. 1. As can be seen from the TEM image, neighboring film caps are clearly interconnected at the contact areas, resulting in direct magnetic exchange coupling. The coupling strength, however, will strongly depend on the Py thickness. It is expected that this coupling might influence the in-plane circulation orientation of connected caps, leading to frustration in a hexagonal cap array [44, 45] or even to the formation of anti-vortices [49, 50] at the contact area when the circulations are contra-rotating. Please note that due to the curved particle surface, the thickness of the deposited Py layer in radial direction decreases from the top center of the film cap towards the rim, thus the vortex core area is expected to be enlarged compared to planar vortex structures.

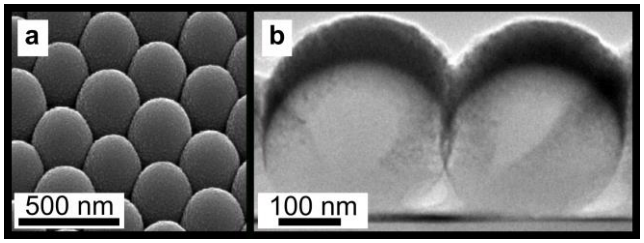

Figure 1:(a) SEM image of an array of densely packed silica particles with diameters of 330 nm covered by a 70-nm-thick Py layer . The image was taken under an angle of 30° with respect to the sample normal. (b) Corresponding cross section TEM image.

For all samples in-plane MOKE hysteresis loops were recorded at room temperature as presented in Fig. 2. Interestingly, only caps with a Py thickness smaller than 100 nm show the typical vortex characteristics, whereas for the 100-nm-thick structures a clear transition to a different magnetic configuration appears, which will be discussed later.

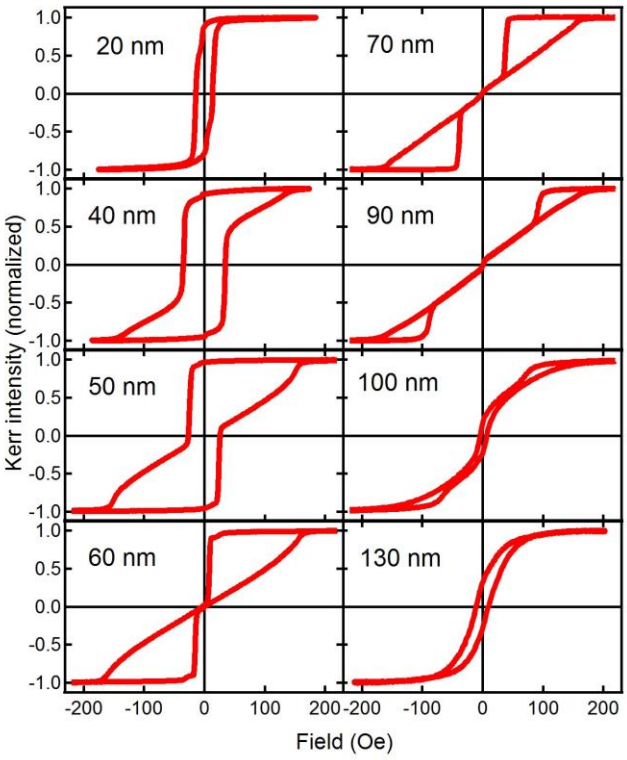

Figure 2: In-plane MOKE hysteresis loops of Py caps with different thicknesses measured at room temperature.

From the hysteresis loops the nucleation and annihilation fields were extracted for samples with Py thicknesses below 100 nm. As summarized in Fig. 3, it is apparent that a transition from a negative to a positive nucleation field occurs for a Py thickness between 50 nm and 60 nm, while the annihilation field only shows a slight variation. The increase of the nucleation field can be explained by the increasing magnetic moment of the caps with Py thickness, which is the driving force of the vortex formation. However, intercap dipolar interactions opposing vortex nucleation [38] and exchange coupling between neighboring caps promoting vortex nucleation as will be shown later need to be taken into account as well.

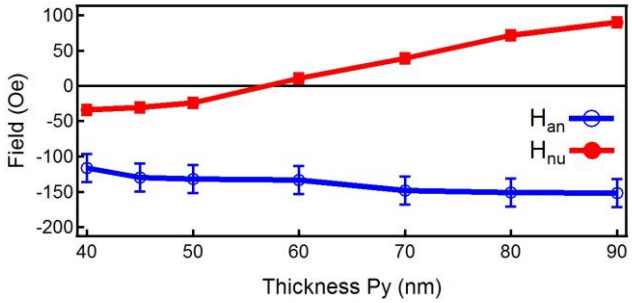

Figure 3: Dependence of H_{nu} and H_{an} for Py caps with different thicknesses measured at room temperature.

Furthermore, the temperature dependence of the annihilation and nucleation field was investigated by MOKE magnetometry for the 70-nm-thick Py cap array. In Fig. 4a the temperature

dependence of the nucleation field is shown for temperatures between 100 K and 500 K. It is apparent that by decreasing the temperature a slight increase of the nucleation field is observed. Please note that the values obtained at room temperature shows a slight difference in comparison with the thickness series presented in Fig. 3 as these measurements were performed on a different but comparable sample.

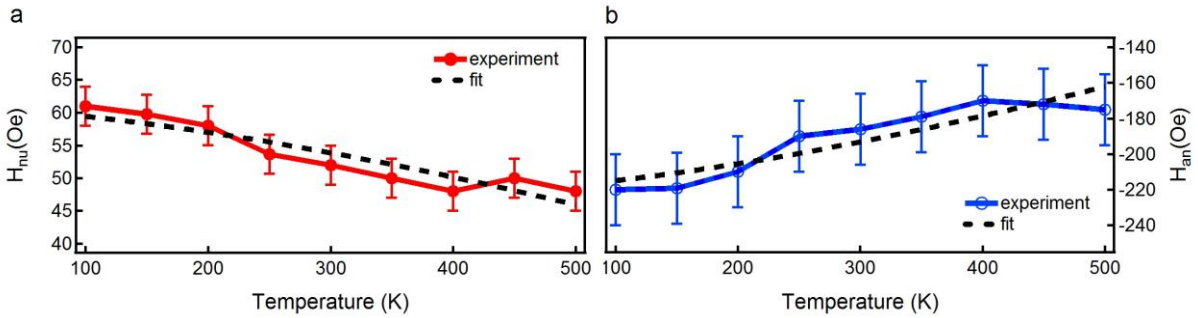

Figure 4: Temperature dependence of (a) H_{nu} and (b) H_{an} for Py caps with a thickness of 70 nm.

On the other hand, the annihilation field, shown in Fig. 4b, increases with decreasing temperature. Please note that both fields reveal a similar relative change with temperature, indicating the stabilization of a vortex state at lower temperatures. As H_{nu} and H_{an} are proportional to the saturation magnetization [9, 51, 52], the temperature dependence can be simulated using the following relationship: $H_{an,nu}(T) = H_{(an,nu)0}\ (1-\alpha_{an,\ nu}T^{3/2})$. The corresponding fits are included in Fig. 4 (dashed lines) using the following parameters, $\alpha_{an}= (2.35 \pm 0.35) \times 10^{-5}\ K^{-3/2}$ and $\alpha_{nu}= (2.18 \pm 0.29) \times 10^{-5}\ K^{-3/2}$. A similar behavior was also reported for planar Py disk structures with a diameter of 526 nm [9].

Due to the expected strong exchange coupling of the vortex states in the two-dimensional lattice, a correlation of the circulation sense between neighboring Py caps might be expected. To tackle this question and to follow the reversal behavior of the vortex lattice, in particular the in-plane circulation, high resolution MTXM imaging was performed. The magnetization-reversal process of 50-nm-thick Py caps was imaged with varying magnetic in-plane fields. Please note that instead of SiO particles, polystyrene particles of comparable size (300 nm) have been used, which were prepared on a 100-nm-thick silicon-nitride membrane to allow for sufficient transmission of soft x-rays. A sequence of typical domain structures starting from in-plane saturation (at magnetic field of 130 Oe) and lowering the fields down to 90 Oe are shown in Fig. 5a. By slightly reducing the magnetic field to 120 Oe, we were able to see the onset of vortex nucleation. In this geometry, the dark/bright contrast on the caps indicates the projection of the local Fe magnetization along the photon propagation direction of circularly polarized photons. Consequently, the curling in-plane domain structure, which rotates either clockwise or counter-clockwise, is clearly visible. By further reducing the field, the nucleation proceeds, but surprisingly, via domain wall propagation and not by individual and randomly distributed nucleation events. By analyzing the rotation sense of the reversed areas, it turned out that

large connected areas exist with the same circulation sense as shown in Fig. 5. This behavior clearly confirms the presence of direct exchange coupling between neighboring caps.

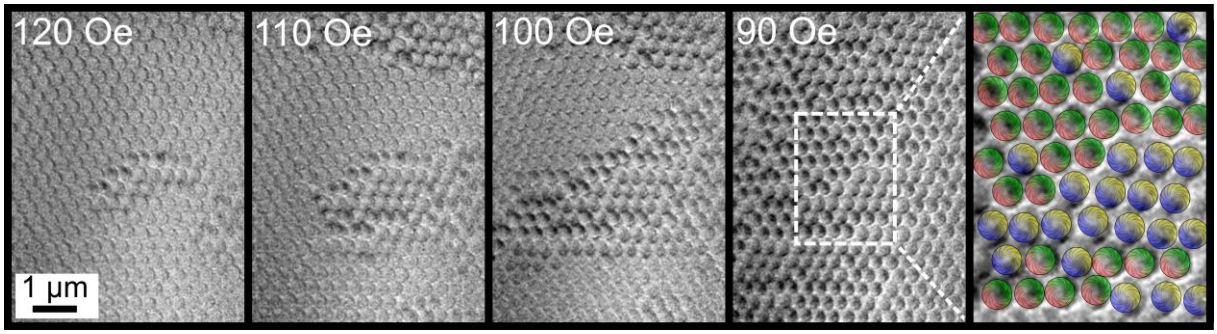

Figure 5: MTXM image of a two dimensional vortex lattice formed on 300 nm polystyrene particles covered by a 50-nm thick Py film. In the right image, which is an enlargement of the MTXM image taken at 90 Oe, the rotation sense of the in-plane circulations are color coded, revealing clearly large domains with same circulation.

To further investigate the vortex structures, in particular the vortex cores, two samples with different Py thicknesses (45 nm; 130 nm) were imaged by SMRM, which allows imaging the vortex cores directly. In Fig. 6a the SMRM image of a vortex array with a Py thickness of 45 nm in the demagnetized state is shown. The light and dark areas located in the cap centers reveal directly the vortex cores. For a better illustration the boundaries of some particles are marked. Please note that the cores are distributed randomly and no distinct contrast is seen from the circulation as expected from the spherical shape of the particles. Afterwards, the vortex core movement was probed by applying an in-plane magnetic field of 167 Oe, which results in lateral displacements of the vortex cores (not shown). By comparing carefully both images and extracting the difference in lateral core displacement, the sense of rotation (circulation) of the in-plane magnetic moment configuration can be determined as marked by the color coding of the caps in Fig. 6a. In this regard, recent theoretical calculations suggested that in thin spherical caps a polarity-chirality coupling should occur for topological reasons [53], which might be expressed in a preferred polarity orientation for vortices having the same circulation sense. However, at a first glance this was not observed but better statistics are required to draw a clear conclusion.

Additionally, the absolute core displacements, including its directions, is presented in a polar plot (Fig. 6b), revealing a rather homogeneous distribution perpendicular to the applied field direction. In contrast, a much broader distribution with larger displacements is observed for the sample with a Py thickness of 130 nm (Fig. 6d). We believe that this effect is connected to the appearance of strong exchange coupling between neighboring caps. For instance, for the sample with the thicker Py layer, indeed a broader distribution is expected as the displacement now depends also on the displacement of

neighboring caps affecting each other. In addition, for the thick Py layer the magnetostatic coupling is increased as well. It is also interesting to note that the cores appear much larger (see Fig. 6c) in comparison to the caps with a Py thickness of 45 nm. This lateral expansion of the core area is due to the curvature of the Py surface and will scale with the Py thickness. In addition, the presence of more aligned c-states might be indicated in the image as well. Initially, we were not expecting vortex structures when looking at the corresponding hysteresis loop (Fig. 3). But it seems that the reduction in in-plane magnetization when lowering the field from saturation is now also initiated by the nucleation of out-of-plane vortex cores and in combination with the presence of c-states the observed loop shape can be explained as supported by micromagnetic simulations [45].

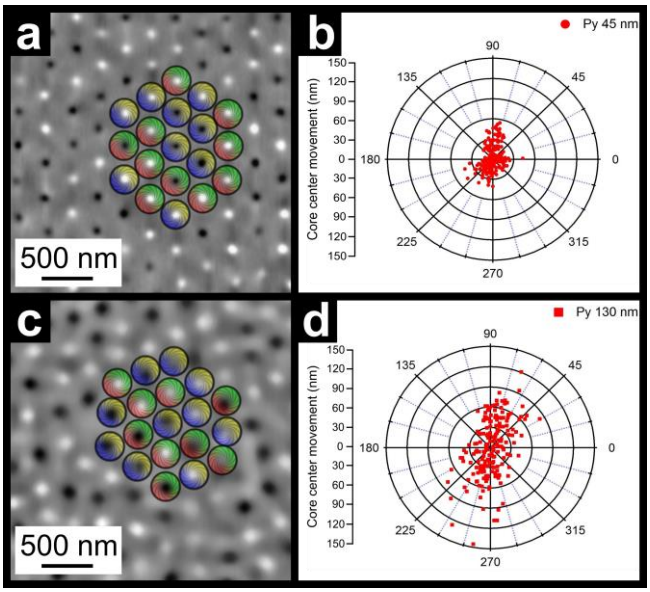

Figure 6: SMRM images of a vortex array with a Py thickness of (a) 45 nm and (c) of 130 nm in the demagnetized state. The bright and dark spots in the center of the Py caps correspond to the magnetization orientation of the vortex cores pointing either up or down. By comparing the lateral core positions with and without an external in-plane field of 16.7 mT, a pole-diagram was created for both samples (b, d), showing the lateral displacement of the cores mainly perpendicular to the applied field direction (along 0 degree direction).

In conclusion, the magnetization reversal of magnetic vortices in a two-dimensional lattice was investigated for various Py thicknesses and as function of temperature up to 500 K. It was shown that by increasing the Py cap thickness or lowering the temperature, both critical fields, nucleation and annihilation field, increase. Furthermore, the onset of exchange coupling between neighboring caps was as well indicated by an increased nucleation field. The nucleation process itself was directly imaged by full-field magnetic soft x-ray microscopy, which confirmed that nucleation does not occur by individual and randomly distributed nucleation events but arises via domain wall propagation due to coupling. By analyzing the rotation sense of the reversed areas, it turned out that large connected

domains exist with the same circulation sense. In a further study, an in-field scanning magnetoresistance microscope was employed to image the vortex cores and to probe the lateral core displacements when an in-plane field is applied, revealing spatially enlarged vortex cores and a broader distribution with increasing Py layer thickness. In addition, the presence of some mixed states, vortices and c-states, is indicated for the array with the thickest Py layer.

Acknowledgement

The authors acknowledge B. Knoblich (University of Augsburg) for TEM sample preparation. S. Thomas kindly acknowledges the financial support provided by the Department of Science and Technology, India, via the INSPIRE Faculty award.

References

1. R. P. Cowburn, D. K. Koltsov, A. O. Adeyeye, M. E. Welland, and D. M. Tricker, Phys. Rev. Lett. 83, 1042 (1999).

2. N. A. Usov and S. E. Peschany, J. Magn. Magn. Mater. 118, 290 (1993).

3. A. Wachowiak, J. Wiebe, M. Bode, O. Pietzsch, M. Morgenstern, and R. Wiesendanger, Science 18, 577 (2002).

4. K. L. Metlov and Young Pak Lee, J. Appl. Phys.113, 223905 (2013).

5. S.-H. Chung, R. D. McMichael, D. T. Pierce, and J. Unguris, Phys. Rev. B 81, 024410 (2010).

6. B. Van Waeyenberge, A. Puzic, H. Stoll, K. W. Chou, T. Tyliszczak, R. Hertel, M. Fähnle, H. Brückl, K. Rott, G. Reiss, I. Neudecker, D. Weiss, C. H. Back, and G. Schütz, Nature 444, 461 (2006).

7. T. Shinjo, T. Okuno, R. Hassdorf, K. Shigeto, and T. Ono, Science 289, 930 (2000).

8. K. Y. Guslienko, V. Novosad, Y. Otani, H. Shima, and K. Fukamichi, Appl. Phys. Lett. 78, 3848 (2001).

9. G. Mihajlovic, M. S. Patrick, J. E. Pearson, V. Novosad, S. D. Bader, M. Field, G. J. Sullivan, and A. Hoffmann, Appl. Phys. Lett. 96, 112501 (2010).

10. K. M. Lebecki and U. Nowak, J. Appl. Phys. 113, 023906 (2013).

11. E. Östman, U. B. Arnalds, E. Melander, V. Kapaklis, G. K. Pálsson, A. Y. Saw, M. A. Verschuuren, F. Kronast, E. Th. Papaioannou, C. S. Fadley, and B. Hjörvarsson, New J. Phys. 16, 053002 (2014)

12. A. Neudert, J. McCord, R. Sch€afer, and L. Schultz, J. Appl. Phys. 97, 10E701 (2005).

13. R. Hertel, S. Gliga, M. F€ahnle, and C. M. Schneider, Phys. Rev. Lett. 98, 117201 (2007).

14. Brückl, K. Rott, G. Reiss, I. Neudecker, D. Weiss, C. H. Back, and G. Schütz, Nature 444, 461 (2006).

15. A. Vansteenkiste, K. W. Chou, M. Weigand, M. Curcic, V. Sackmann, H. Stoll, T. Tyliszczak, G. Woltersdorf, C. H. Back, G. Schütz, and B. Van Waeyenberge, Nat. Phys. 5, 332 (2009).

16. M. Weigand, B. Van Waeyenberge, A. Vansteenkiste, M. Curcic, V. Sackmann, H. Stoll, T. Tyliszczak, K. Kaznatcheev, D. Bertwistle, G. Woltersdorf, C. H. Back, and G. Sch€utz, Phys. Rev. Lett. 102, 077201 (2009).

17. K. Yamada, S. Kasai, Y. Nakatani, K. Kobayashi, and T. Ono, Appl. Phys. Lett. 93, 152502 (2008).

18. V. S. Pribiag, I. N. Krivorotov, G. D. Fuchs, P. M. Braganca, O. Ozatay, J. C. Sankey, D. C. Ralph, and R. A. Buhrman, Nat. Phys. 3, 498 (2007).

19. R. Moriya, L. Thomas, M. Hayashi, Y. B. Bazaliy, C. Rettner, and S. S. P. Parkin, Nat. Phys. 4, 368 (2008).

20. K. Yamada, S. Kasai, Y. Nakatani, K. Kobayashi, H. Kohno, A. Thiaville, and T. Ono, Nature Mater. 6, 270 (2007).

21. R. Rückriem, T. Schrefl, and M. Albrecht, Appl. Phys. Lett. 104, 052414 (2014).

22. A. Thiaville, J. M. Garcia, R. Dittrich, J. Miltat, and T. Schrefl, Phys. Rev. B 67, 094410 (2003).

23. N. Kikuchi, S. Okamoto, O. Kitakami, and Y. Shimada, J. Appl. Phys. 90, 6548 (2001).

24. J. G. S. Lok, A. K. Geim, J. C. Maan, S. V. Dubonos, L. Theil Kuhn, and P. E. Lindelof, Phys. Rev. B 58, 12201 (1998).

25. D. Mitin, D. Nissen, P. Schädlich, S. S. P. K. Arekapudi, and M. Albrecht, J. Appl. Phys. 115, 063906 (2014).

26. S. Sugimoto, Y. Fukuma, S. Kasai, T. Kimura, A. Barman, and Y. Otani, Phys. Rev. Lett. 106, 197203 (2011).

27 A. Vogel, T. Kamionka, M. Martens, A. Drews, K. W. Chou, T. Tyliszczak, H. Stoll, B. Van Waeyenberge, and G. Meier, Phys. Rev. Lett. 106, 137201 (2011).

28. A. Vogel, A. Drews, M. Weigand, and G. Meier, AIP Adv. 2, 042180 (2012).

29. H. Jung, K.-S. Lee, D.-E. Jeong, Y.-S. Choi, Y.-S. Yu, D.-S. Han, A. Vogel, L. Bocklage, G. Meier, M.-Y. Im, P. Fischer, and S.-K. Kim, Sci. Rep. 1, 59 (2011).

30. D.-S. Han, A. Vogel, H. Jung, K.-S. Lee, M. Weigand, H. Stoll, G. Schütz, P. Fischer, G. Meier, and S.-K. Kim, Sci. Rep. 3, 2262 (2013).

31. J. Shibata and Y. Otani, Phys. Rev. B 70, 012404 (2004).

32. A. Y. Galkin, B. A. Ivanov, and C. E. Zaspel, Phys. Rev. B 74, 144419 (2006).

33. A. Vogel, M. Hänze, A. Drews, and G. Meier, Phys. Rev. B 89, 104403 (2014).

34. M. Hänze, C. F. Adolff, M. Weigand, and G. Meier, Appl. Phys. Lett. 104, 182405 (2014).

35. C. F. Adolff, M. Hänze, A. Vogel, M. Weigand, M. Martens, and G. Meier, Phys. Rev. B 88, 224425 (2013).

36. O. V. Sukhostavets, J. Gonzalez, and K. Y. Guslienko, Phys. Rev. B 87, 094402 (2013).

37. A. Vogel, A. Drews, T. Kamionka, M. Bolte, and G. Meier, Phys. Rev. Lett. 105, 037201 (2010).

38. J. Mejía-López, D. Altbir, A. H. Romero, X. Batlle, I. V. Roshchin, C.-P. Li, and I. K. Schuller, J. Appl. Phys. 100, 104319 (2006).

39. A. Yu. Galkin, B. A. Ivanov, and C. E. Zaspel, Phys. Rev. B 74, 144419 (2006).

40. M. Albrecht, G. Hu, I. L. Guhr, T. C. Ulbrich, J. Boneberg, P. Leiderer, and G. Schatz, Nat. Mat. 4, 203 (2005).

41. R. Streubel, L. Han, M.-Y. Im, F. Kronast, U. K. Röler, F. Radu, R. Abrudan, G. Lin, O. G. Schmidt, P. Fischer, and D. Makarov, Scientific Reports 5, 8787 (2015).

42. S. Thomas, D. Nissen, and M. Albrecht, Appl. Phys. Lett. 105, 022405 (2014).

43. R. Streubel, V.P. Kravchuk, D. D. Sheka, D. Makarov, F. Kronast, O.G. Schmidt, and Y. Gaididei, Appl. Phys. Lett. 101, 132419 (2012).

44. R. Streubel, D. Makarov, F. Kronast, V. Kravchuk, M. Albrecht, and O. G. Schmidt, Phys. Rev. B 85, 174429 (2012).

45. M. V. Sapozhnikov, O. L. Ermolaeva, B. G. Gribkov, I. M. Nefedov, I. R. Karetnikova, S. A. Gusev, V. V. Rogov, B. B. Troitskii, and L. V. Khokhlova, Phys. Rev. B 85, 054402 (2012).

46. R. Micheletto, H. Fukuda, and M. Ohtsut, Langmuir 11, 3333 (1996).

47. P. Fischer, IEEE Trans. Magn. 51, 1 (2015).

48. A. Moser, D. Weller, M. E. Best, and M. F. Doerner, J. Appl. Phys. 85, 5018 (1999).

49. A. Ruotolo, V. Cros, B. Georges, A. Dussaux, J. Grollier, C. Deranlot, R. Guillemet, K. Bouzehouane, S. Fusil, and A. Fert, Nature Nanotechnology 4, 528 - 532 (2009).

50. H.-B. Jeong, and S.-K. Kim, Appl. Phys. Lett. 105, 222410 (2014)

51. V. Novosad, K. Yu. Guslienko, H. Shima, Y. Otani, K. Fukamichi, N. Kikuchi, O. Kitakami, and Y. Shimada, IEEE Trans. Magn. 37, 2088 (2001).

52. K. Y. Guslienko, V. Novosad, Y. Otani, H. Shima, and K. Fukamichi, Phys. Rev. B. 65, 024414 (2001).

53. V. P. Kravchuk, D. D. Sheka, R. Streubel, D. Makarov, O. G. Schmidt, and Y. Gaididei, Phys. Rev. B 85, 144433 (2012).